



# IV

## Publication IV

O. Reentilä, M. Mattila, M. Sopanen, and H. Lipsanen, *In-situ determination of In-GaAs and GaAsN composition in multi-quantum-well structures*, Journal of Applied Physics **101** 033533 (2007)

© 2007 American Institute of Physics

Reprinted with permission.

## ***In situ* determination of InGaAs and GaAsN composition in multiquantum-well structures**

O. Reentilä,<sup>a)</sup> M. Mattila, M. Sopanen, and H. Lipsanen

*Optoelectronics Laboratory, Micronova, Helsinki University of Technology, P. O. Box 3500, FIN-02015 TKK, Finland*

(Received 28 August 2006; accepted 7 December 2006; published online 14 February 2007)

Metal-organic vapor phase epitaxial growth of InGaAs/GaAs and GaAsN/GaAs multiquantum-well (MQW) structures was monitored by *in situ* reflectometry at 635 nm using a normal incidence reflectance setup. The reflectance signal is found to change significantly during both quantum-well (QW) and barrier growth regions. A matrix method is used to calculate the theoretical reflectance curve and comparing the theoretical curves to the measured ones the complex refractive index of the ternary alloys are derived. Consequently, when the behavior of the complex refractive indices of InGaAs and GaAsN is known as a function of composition, the composition of all the QWs in the MQW structure can be determined *in situ*. © 2007 American Institute of Physics.

[DOI: [10.1063/1.2435065](https://doi.org/10.1063/1.2435065)]

### **I. INTRODUCTION**

The *in situ* monitoring of metal-organic vapor phase epitaxial (MOVPE) growth of semiconductor structures has proven to be an efficient tool in the fabrication technology. MOVPE growth of thick layers or layer stacks, e.g., Bragg reflectors, can be monitored with a simple reflectometer setup.<sup>1–3</sup> There are also reports which show that the quality and composition or growth rate of the layers can be determined by *in situ* reflectance measurements, see, for example (Refs. [4–7]). The report of Lum *et al.*<sup>8</sup> showed that by choosing a suitable wavelength growth of very thin layers, such as quantum wells (QWs), can also be observed *in situ*. This report was published already in 1996, but the use of *in situ* reflectometer data in determining the compositions of thin layers was reported only recently.<sup>9,10</sup>

Here we use *in situ* reflectometry measurements and theoretically calculated reflectance curves to determine the high-temperature complex refractive indices of InGaAs and GaAsN as a function of indium and nitrogen contents, respectively. Along these results, the field of application of the *in situ* reflectance method is expanded to cover multiquantum-well (MQW) structures. The *in situ* determination of the composition for each QW is made possible, even if the compositions vary from one QW to another within the structure.

### **II. EXPERIMENT**

All the samples were fabricated by a vertical low-pressure MOVPE system using hydrogen (H<sub>2</sub>) as a carrier gas. The rotation speed of the susceptor was 100 rpm and total flow to the reactor 6 slm. Trimethylindium (TMIn), trimethylgallium (TMGa), tertiarybutylarsine (TBAs), and dimethylhydrazine (DMHz) were used as precursors for indium, gallium, arsenic, and nitrogen, respectively. The growth temperature for all the QW structures, 575 °C (a ther-

mocouple reading), is a typical growth temperature for dilute nitride materials in our reactor. All the layer structures were grown on semi-insulating 350- $\mu$ m-thick (100)-oriented GaAs substrates.

InGaAs samples consisted of three 7-nm-thick InGaAs QWs spaced with 13-nm-thick GaAs barrier layers. The indium contents of the QWs were 7, 12, 15, 17, 19, 23, and 27 %. The growth pressure for the InGaAs MQW samples was 100 Torr.

GaAsN samples consisted of four GaAsN QWs spaced with GaAs barriers. Due to the different growth pressures (100, 300, and 700 Torr) used for the samples the layer thicknesses vary in the ranges of 7–10 and 16–23 nm for QWs and barriers, respectively. The nitrogen content was 2–5% depending on the growth parameters.

To determine the complex refractive index ( $n_{\text{complex}} = n + i\kappa$ ) of GaAs, thick GaAs layers were fabricated on 270-nm-thick Al<sub>0.89</sub>Ga<sub>0.11</sub>As buffers. AlGaAs layers were always grown at 690 °C and the growth temperatures of the GaAs bulk layers were 575, 620, and 670 °C.

The *in situ* reflectance measurements were performed with a normal incidence reflectance setup using a halogen lamp as the light source and with a reflectance detection wavelength of 635 nm. The used wavelength is absorbed by both studied material systems, InGaAs and GaAsN. This, however, does not prevent the use of *in situ* monitoring as a method to examine both these systems. Calculated from  $\kappa = -0.4$  (Ref. 5) the penetration depth to GaAs layers at 635 nm is about 250 nm. As a matter of fact, absorption of the light used for *in situ* monitoring is a necessary requirement in the case of thin layer structures. This will be shown later on by calculations and experimental data.

The post-growth characterization of the MQW samples was done by high-resolution x-ray diffractometer measurements (HR-XRD) and simulations. The measurements were performed in  $\omega-2\theta$  configuration. In the case of ternary alloy samples containing several QWs we consider XRD as a suitable and reliable method to determine the QW and barrier

<sup>a)</sup>Electronic mail: [outi.reentila@tkk.fi](mailto:outi.reentila@tkk.fi)

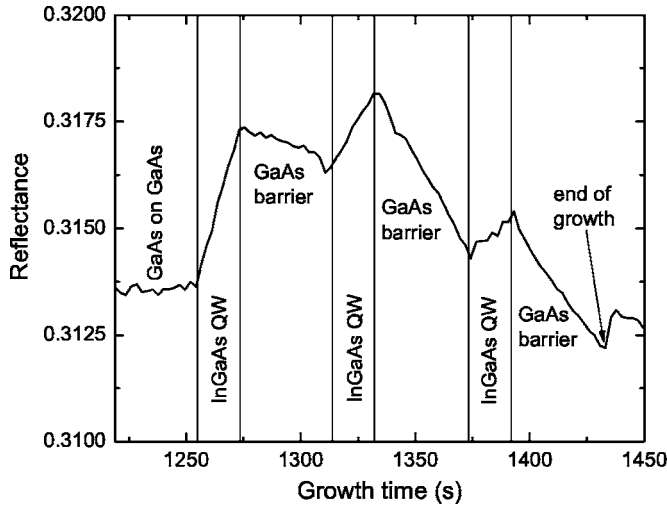


FIG. 1. Typical reflectance data measured during the growth of an InGaAs/GaAs MQW structure. The QW and barrier growth regions are denoted in the figure. The indium content of the InGaAs layers was 19.4%.

thicknesses, as well as the compositions of the QWs. Also the bulk GaAs-on-AlGaAs samples were characterized by HR-XRD. The quality of the MQW samples was confirmed by photoluminescence (PL) measurements, although the results are not shown here.

### III. RESULTS AND DISCUSSION

Figure 1 shows the *in situ* reflectance data measured during MOVPE growth of a  $\text{In}_{0.19}\text{Ga}_{0.81}\text{As}/\text{GaAs}$  MQW structure. The QW and barrier growth regions are denoted in the figure. It is shown in the figure that the reflectance change during the QW growth is positive ( $\Delta R > 0$ ) and during the growth of the barriers it is negative ( $\Delta R < 0$ ). The complex refractive index differences between the QWs and barriers cause the changes in the reflectances and also enable the *in situ* characterization of the MQW structure. In the case of these GaAs based ternary alloys InGaAs and GaAsN, the refractive index difference between GaAs and the alloy material naturally increases as the N or In content of the alloy increases.

#### A. Calculation of the theoretical reflectance curves

Due to the small thickness of the quantum well and the barrier layers, no complete Fabry-Pérot oscillations can be observed in the reflectance curves measured during growth of the MQW structures. Therefore, to enable the extraction of the real and imaginary parts of the complex refractive index for each layer, the measured data was compared with theoretical reflectance curves. The well-known matrix method was used to calculate the reflectance of the multilayer structure for given layer thicknesses, i.e., at a given time of growth. To get the time evolution of the reflectance, the thickness of the topmost layer was increased according to the actual growth rate. Thus, the parameters needed for the calculations are the growth rate, the growth time, and the complex refractive index of each layer. In this work, the growth rates were calculated from XRD measurement results, and to reduce the number of free parameters, the complex refractive

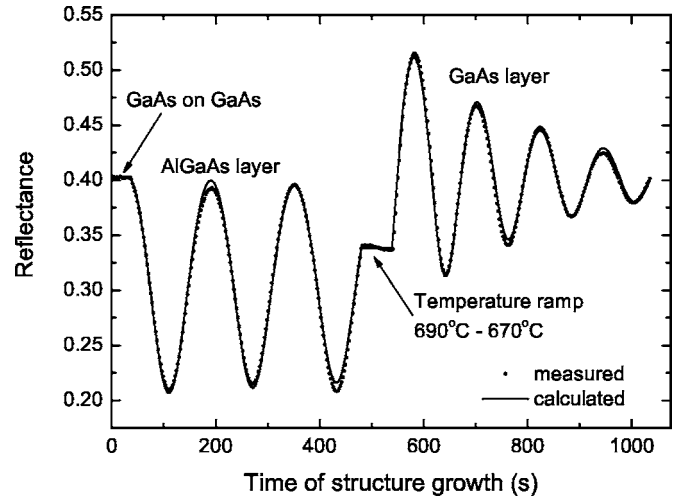


FIG. 2. Measured (dotted line) and calculated (solid line) reflectance of the GaAs-on-AlGaAs test structure used to determine  $n$  and  $\kappa$  of GaAs. Values of  $n=3.3$  and  $\kappa=-0.03$  and  $n=4.2$  and  $\kappa=-0.31$  were obtained for  $\text{Al}_{0.89}\text{Ga}_{0.11}\text{As}$  and GaAs, respectively.

index of the GaAs buffer and barriers was fixed. In addition, the calculated curves were normalized so that the reflectance from the GaAs buffer was equal to the measured reflectance. The complex refractive index of the quantum wells was then extracted by fitting the calculation to the measured reflectance data. In the fitting procedure the measured and calculated curves are compared and the best fit has been obtained by least-squares minimization.

The measured reflectance curve and the calculated reflectance for the bulk GaAs reference sample grown at  $670^\circ\text{C}$  are shown in Fig. 2. Because the thickness of the AlGaAs and GaAs layers was large enough, several Fabry-Pérot oscillations can be observed. By fitting procedure, values of  $n=4.2$  and  $\kappa=-0.3$  were obtained for GaAs and similarly  $n=3.3$  and  $\kappa=-0.03$  for AlGaAs. These values are in good agreement with the results reported previously by Breiland and Killeen<sup>4</sup> and Rebey *et al.*<sup>5,6</sup>

To examine the temperature dependence of  $n_{\text{GaAs}}$  and  $\kappa_{\text{GaAs}}$ , bulk GaAs layers on AlGaAs were fabricated also at temperatures of  $575$  and  $620^\circ\text{C}$ . The obtained results are shown in Table I. The accuracy of the values in Table I is estimated to be 2% for  $n_{\text{GaAs}}$  and 10% for  $\kappa_{\text{GaAs}}$ . For these samples the  $n_c$  determination was performed manually from the minima and maxima of the Fabry-Pérot curves. That also explains the large error of  $\kappa$  compared to the error of  $n$ . In the MQW fitting process the value of  $n_{c,\text{GaAs}}$  was fixed to  $4.0-0.3i$ . However, it was observed that a small change in  $n_{c,\text{GaAs}}$  does not influence considerably the determination of QW composition.

TABLE I. Values for  $n_{\text{GaAs}}$  and  $\kappa_{\text{GaAs}}$  obtained from bulk GaAs layers grown at different temperatures (thermocouple readings).

$T_{\text{growth}}$	$n_{\text{GaAs}}$	$\kappa_{\text{GaAs}}$
$575^\circ\text{C}$	4.0	-0.3
$620^\circ\text{C}$	4.1	-0.3
$670^\circ\text{C}$	4.2	-0.3

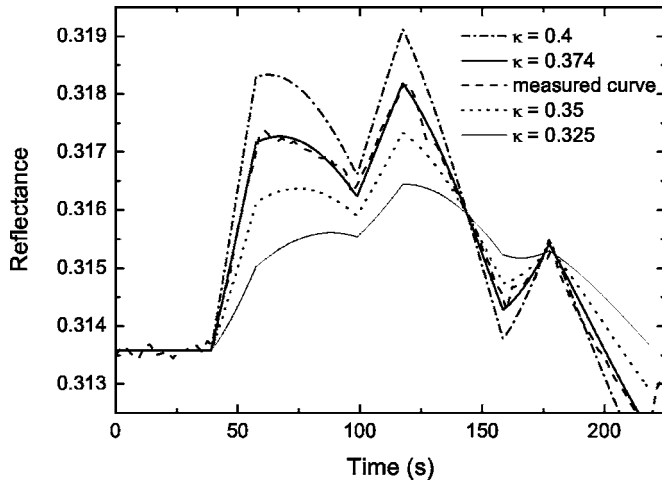


FIG. 3. Measured and calculated reflectance curves of  $\text{In}_{0.19}\text{Ga}_{0.81}\text{As}/\text{GaAs}$  MQW structure.  $n$  was constant with a value of 4.041 and  $\kappa$  was varied from  $-0.325$  to  $-0.4$ .

Figures 3 and 4 show the same measured reflectance curve and several calculated curves with different real and imaginary parts of the complex refractive index. The theoretical reflectance curves in Fig. 3 have been calculated by keeping the value of  $n$  constant at 4.041 while  $\kappa$  was varied from  $-0.325$  to  $-0.4$ . The best fit was achieved with  $\kappa = -0.374$ . Changing the value of  $\kappa$  causes noticeable changes to the amount of the reflectance change ( $\Delta R$ ) during the QW and barrier growth regions. In other words, the different values of  $\kappa$  change the slope  $\Delta R/\Delta t$  measured during growth of the QW and barrier layers.

Correspondingly, the theoretical curves in Fig. 4 were calculated by changing the values of  $n$  between 4.00 and 4.07 and keeping the value of  $\kappa$  at  $-0.374$ . The best correlation between the experimental and theoretical curves was found with  $n=4.041$ . It is worth noticing that the changes in  $n$  do not cause severe changes in the reflectance change ( $\Delta R$ ) caused by the QW or barrier growth, but merely influence the overall level of the reflectance signal of the structure. These different consequences of changes in  $n$  and  $\kappa$  quite

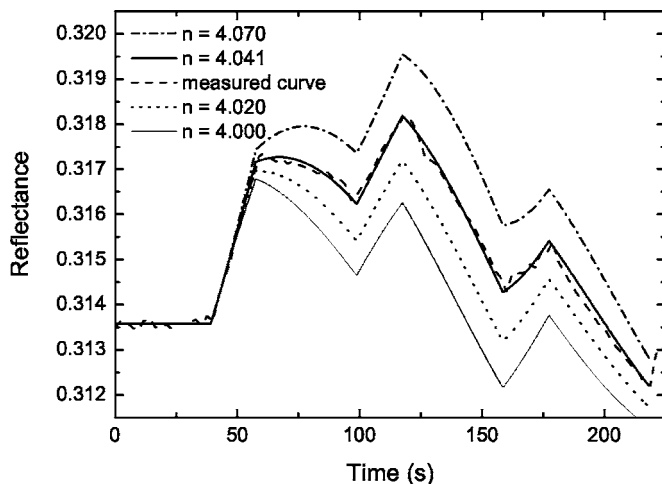


FIG. 4. Measured and calculated reflectance curves of  $\text{In}_{0.19}\text{Ga}_{0.81}\text{As}/\text{GaAs}$  MQW structure.  $\kappa$  was constant with a value of  $-0.374$  while  $n$  was varied between 4.00 and 4.07.

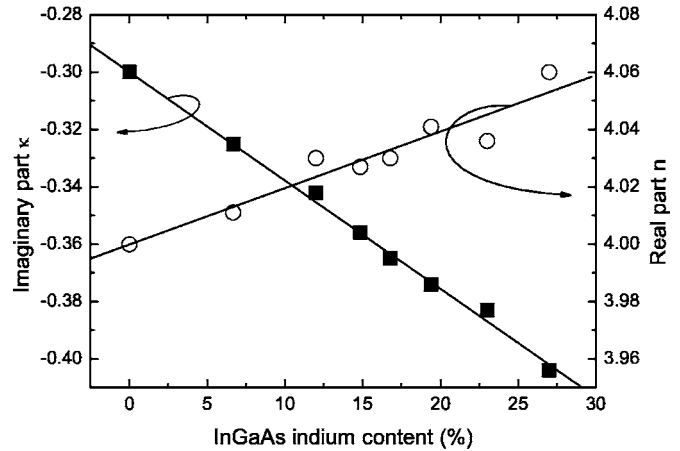


FIG. 5. Measured real part ( $n$ ) and imaginary part ( $\kappa$ ) of the refractive index for InGaAs as a function of the QW indium content. Linear fits to data points are also shown.

naturally enable the independent determination of  $n$  and  $\kappa$ , which, as will be shown later on, can be used when determining the QW compositions *in situ*.

## B. Empirical results and correlation with the model

All the measured reflectance curves were compared with the theoretically calculated curves and a value for  $n_{\text{complex}}$  was obtained for InGaAs and GaAsN as a function of indium and nitrogen content, respectively. Figure 5 shows the real and imaginary parts of the complex refractive index of InGaAs as a function of the QW indium content. In Fig. 5 linear fits forced via the GaAs data points for both  $n$  and  $\kappa$  are shown. The value of  $n$  is increasing and the value of  $\kappa$  decreasing as the indium content increases. The real part  $n_{\text{InGaAs}}$ , as a function of the indium content [In], is given by

$$n_{\text{InGaAs}} = n_{\text{GaAs}} + B_{n,\text{InGaAs}} \cdot [\text{In}], \quad (1)$$

where  $n_{\text{GaAs}}$  is the real part of the refractive index of GaAs and  $B_{n,\text{InGaAs}}$  is a constant with a value of 0.197. Similarly, the imaginary part of the refractive index of InGaAs,  $\kappa_{\text{InGaAs}}$ , as a function of the QW indium content [In] can be written as

$$\kappa_{\text{InGaAs}} = \kappa_{\text{GaAs}} + B_{\kappa,\text{InGaAs}} \cdot [\text{In}], \quad (2)$$

where the constant  $B_{\kappa,\text{InGaAs}}$  has a value  $-0.373$ . The ratio  $B_{\kappa,\text{InGaAs}}/\kappa_{\text{InGaAs}}$  is larger than the ratio  $B_{n,\text{InGaAs}}/n_{\text{InGaAs}}$ , which indicates that the change in indium content causes larger change to the imaginary part of the refractive index of the material than to the real part. In addition, it can be seen from Fig. 5 that the deviation from the linear fit is much smaller for  $\kappa_{\text{InGaAs}}$  than what it is for  $n_{\text{InGaAs}}$ . This is supposed to be caused by the larger change in  $\kappa$  but also by the different nature of  $n$  and  $\kappa$ : it is easier to define the slopes ( $\Delta R/\Delta t$ ) with high reliability than to determine the overall level of the reflectance of the structure. Thus, we suggest that when the indium content of InGaAs QWs is to be determined *in situ*, the use of the relation between  $\kappa_{\text{InGaAs}}$  and indium content is more favorable.

To illustrate the effect of the QW indium content on the reflectance measured during growth, the calculated reflectance curves with indium contents of 5–25% are shown in

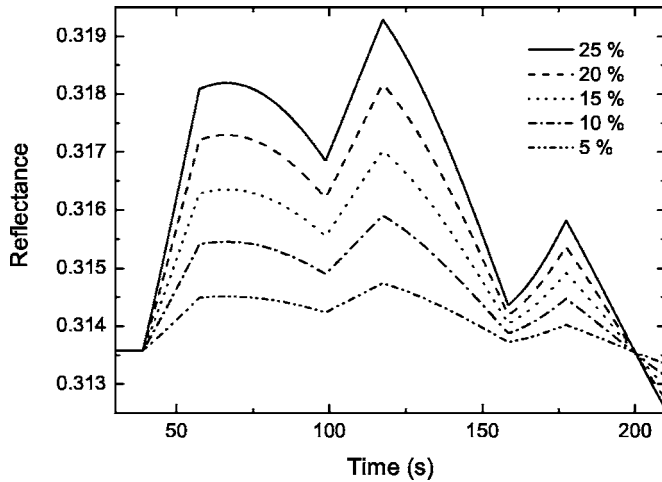


FIG. 6. The calculated reflectance curves for InGaAs/GaAs MQW structures with different QW indium contents. The values of  $n$  and  $\kappa$  have been obtained using Eqs. (1) and (2).

Fig. 6 The values of  $n_{\text{InGaAs}}$  and  $\kappa_{\text{InGaAs}}$  for calculating the reflectance curve for each indium content are taken from Eqs. (1) and (2), respectively.

Figures 7 and 8 show the real part  $n_{\text{GaAsN}}$  and the imaginary part  $\kappa_{\text{GaAsN}}$  of the  $n_{\text{complex,GaAsN}}$  as a function of the GaAsN QW nitrogen content, respectively. Unlike what was observed for InGaAs/GaAs MQWs, the  $n_{\text{GaAsN}}$  does not exhibit any clear trend (either decreasing or increasing), but the data points are somewhat scattered from the GaAs value. It should be noted that GaAsN nitrogen contents of more than 2% are rather large in the dilute nitride range and that such nitrogen contents cause considerable changes in both PL emission energy and in XRD curves. However, here there is no evidence of the dependence of  $n_{\text{GaAsN}}$  on the nitrogen content. Therefore, we assume that nitrogen contents below 5% do not change the refractive index of GaAsN significantly at this relatively high temperature.

In Fig. 8 the  $\kappa_{\text{GaAsN}}$  data points and a linear fit to all the data points are shown. The fit is again forced via the GaAs

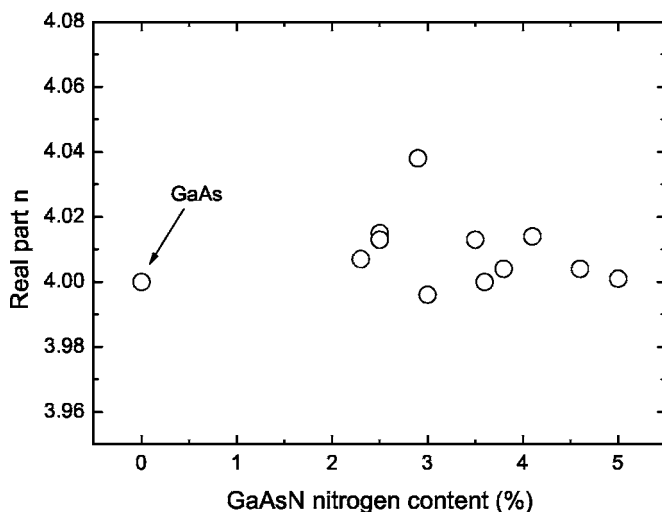


FIG. 7. Measured  $n$  as a function of GaAsN QW nitrogen content. The value of  $n$  does not seem to change much as a function of the QW nitrogen content.

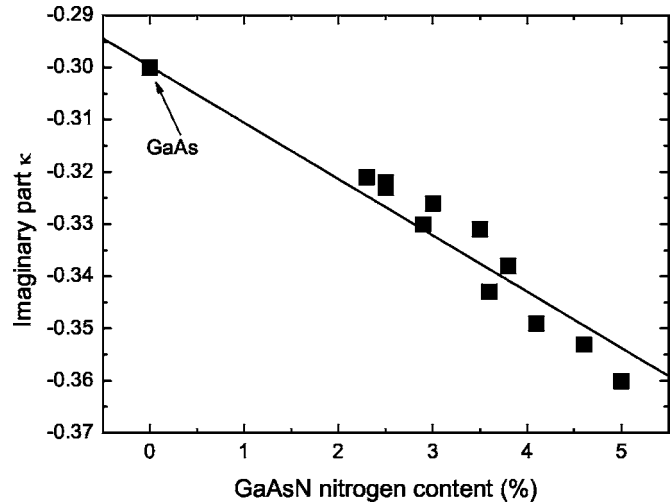


FIG. 8. Measured  $\kappa$  as a function of GaAsN QW nitrogen content. Linear fit to data points is also shown.

data point. Based on the linear fit, an equation for  $\kappa_{\text{GaAsN}}$  can be derived similarly as in the case of InGaAs

$$\kappa_{\text{GaAsN}} = \kappa_{\text{GaAs}} + B_{\kappa,\text{GaAsN}} \cdot [N], \quad (3)$$

where  $B_{\kappa,\text{GaAsN}}$  is a constant with a value of  $-1.078$ .

It is noticeable, that even though the real part of the refractive index does not have significant nitrogen content dependence,  $\kappa_{\text{GaAsN}}$  is strongly dependent on the nitrogen content of GaAsN. The value of  $B_{\kappa,\text{GaAsN}}$  is about three times larger than the corresponding value for InGaAs. This can be explained by the characteristics of dilute nitride materials: Nitrogen is known to change the characteristics, e.g., the band gap, of (In)GaAs considerably already at small percentages, see, for example, Ref. 11. Even if  $n_{\text{GaAsN}}$  does not depend on the nitrogen content, the strong nitrogen content dependence of  $\kappa_{\text{GaAsN}}$  enables the *in situ* monitoring of the quantum-well structures of dilute nitrides.

We would like to emphasize the meaning of these results concerning the *in situ* monitoring of very thin layers and multilayer structures containing very thin layers. When the complex refractive index and the growth rate of a material are known, it is possible to trace the composition of the sample. When studying ternary alloys such as these, the conversion is quite straightforward. Furthermore, the study of the possibilities of this method to characterize the quaternary alloy InGaAsN MQW structures is under way.

In addition to the determination of the layer composition determination, the use of the matrix method enables the analysis of the compositions of such MQW structures in which the QWs are not identical. Therefore, the work done here also provides a tool to determine the composition differences between QWs within the same structure, as long as the growth rate is known.

#### IV. CONCLUSIONS

We have studied the optical *in situ* monitoring of MOVPE grown MQW structures of two GaAs-based ternary alloy systems InGaAs/GaAs and GaAsN/GaAs. *In situ* reflectance measurements combined with the data from the fit-

ting procedure based on the matrix method calculations of the reflectance were used to obtain the high temperature refractive indices of InGaAs and GaAsN at 635 nm. Knowing these parameters enables the *in situ* determination of the nitrogen and indium contents of the quantum wells. In addition, if the growth rate of each QW is known the method enables the determination of the contents of the different QWs in the MQW structure individually.

<sup>1</sup>N. C. Frateschi, S. G. Hummel, and P. D. Dapkus, *Electron. Lett.* **27**, 155 (1991).

<sup>2</sup>K. D. Choquette and H. Q. Hou, *Proc. IEEE* **85**, 1730 (1997).

<sup>3</sup>J.-H. Baek, B. Lee, W. S. Han, H. K. Cho, J. M. Smith, and I. H. Choi, *Jpn. J. Appl. Phys., Part 1* **38**, 2707 (1999).

<sup>4</sup>W. G. Breiland and K. P. Killeen, *J. Appl. Phys.* **78**, 6726 (1995).

<sup>5</sup>A. Rebey, M. M. Habchi, A. Bchetnia, and B. El Jani, *J. Cryst. Growth* **261**, 450 (2004).

<sup>6</sup>A. Rebey, M. M. Habchi, Z. Benzarti, and B. El Jani, *Microelectron. J.* **35**, 179 (2004).

<sup>7</sup>C. Wataani, Y. Hanamaki, M. Takemi, K. Ono, Y. Mihashi, and T. Nishimura, *J. Cryst. Growth* **281**, 227 (2005).

<sup>8</sup>R. M. Lum, M. L. McDonald, J. C. Bean, J. Vandenberg, T. L. Pernell, S. N. G. Chu, A. Robertson, and A. Karp, *Appl. Phys. Lett.* **69**, 928 (1996).

<sup>9</sup>O. Reentilä, M. Mattila, M. Sopanen, and H. Lipsanen, *J. Cryst. Growth* **290**, 345 (2006).

<sup>10</sup>O. Reentilä, M. Mattila, L. Knuutila, T. Hakkarainen, M. Sopanen, and H. Lipsanen, *J. Appl. Phys.* **100**, 013509 (2006).

<sup>11</sup>M. Kondow, K. Uomi, A. Niwa, T. Kitatani, S. Watahiki, and Y. Yazawa, *Jpn. J. Appl. Phys., Part 1* **35**, 1273 (1996).